Optik 125 (2014) 4417–4421

Contents lists available at ScienceDirect

Optik

journal homepage: www.elsevier.de/ijleo

The impacts of temperature and emissivity estimations on radiance-based calibration for HJ-1B/IRS TIR band

JiaGuo Li[a,b], XingFa Gu[a,b], LiMin Zhao[a,b,*], Yong Xie[a,b], Hui Gong[a,b], Dong Wang[a,b]

[a] State Key Laboratory of Remote Sensing Science, Jointly Sponsored by the Institute of Remote Sensing and Digital Earth of Chinese Academy of Sciences and Beijing Normal University, Beijing 100101, China
[b] Institute of Remote Sensing and Digital Earth, Chinese Academy of Sciences, Beijing 100101, China

ARTICLE INFO

Article history:
Received 8 August 2013
Accepted 20 February 2014

Keywords:
Remote sensing
Vicarious calibration
HJ
IRS

ABSTRACT

The IRS radiometer on the HJ-1B satellite of HJ-1 constellation has just a wide band (IRS B08) in thermal infrared spectral region between 10 and 12 μm. The onboard radiometric calibration of IRS B08 is implemented by periodically heating the blackbody of calibration system from normal temperature status (NTS) to high temperature status (HTS) for the lack of observation to deep space. Radiance-based vicarious calibration was taken as one point in two-point calibration method to substitute NTS for the instability of NTS. The estimation impacts of temperature and emissivity were analyzed by defining band matching factor *k*. The results indicate that their impacts were related to channel center wavelengths of reference and target bands. As to the reference band of CE312 B02, temperature impact of ±10 K estimated error on IRS B08 TOA radiance can be ignored while six substituted emissivities demonstrated their impacts can also be ignored. However, if CE312 B03 or B04 was taken as reference bands, the impacts cannot be ignored even emissivity-specimens of fresh water, sea water and blackbody were used as actual surface. Linear combination of two reference bands surrounding target band, such as CE312 B03 and B04 to IRS B08, significantly reduced the calibration uncertainty of using single reference band from 1.8 K and 2.5 K to 0.4 K. The vicarious calibration accuracy based on CE312 B02 is 0.25 K and the vicarious calibration coefficients could be used from August 2009 to August 2010.

1. Introduction

Radiometric calibration is prerequisite for quantitative applications of remote sensing [1]. Vicarious calibration (VC) is an effective way to implement radiometric calibration in which calibrated ground-based or airborne radiometers deployed on or above a spectrally and spatially homogeneous target take simultaneous measurements during the periods of aircraft or satellite instruments overpass [2]. VC can be performed in the thermal infrared spectral region using temperature-based approach or/and radiance-based approach [3]. It is necessary to measure field surface temperature and emissivity in temperature-based method with rigorous experimental condition and operation, and to match spectral response functions between *in situ* radiometer and target sensor indispensably for radiance-based method [4]. This study presents the estimation for the optimal selection of reference bands and band matching affection on calibration accuracy for IRS B08 using measurements from site campaigns at Lake Qinghai, west China, to improve its level of quantitative applications.

2. HJ-1B/IRS

2.1. Overview

HJ-1B is one of the satellites of the HJ-1 constellation launched in September 2008 that designed for Chinese environmental protection and disaster monitor [5]. The IRS instrument on the HJ-1B satellite is characterized with high spatial resolution and four-band multispectral resolution. The IRS instrument consists of three subsystems according to spectral range: the near-infrared (NIR), the mid-wave infrared (MWIR), and the thermal infrared (TIR). The thermal infrared, discussed in this study, has just a broad band (B08) with a spatial resolution of 300 m and a swath width of 720 km. Table 1 gives the summary characteristics of the TIR band.

2.2. Onboard calibration

The TIR subsystem has an onboard calibration system (OCS) based on blackbody for converting the digital numbers measured

* Corresponding author at: No. 20, Datun Road, Chaoyan District, Beijing City, China. Tel.: +86 1064839949; fax: +86 1064839949.
E-mail address: jacoli@126.com (L. Zhao).

http://dx.doi.org/10.1016/j.ijleo.2014.02.037
0030-4026/

Table 1
HJ-1B/IRS TIR summary characteristics.

Spatial resolution	Swath width	Signal quantization levels	NEΔT	Band pass
300 m	720 km	10 bits	0.38 K	10.6–12.6 μm

by the subsystem to calibrated radiance using formula (1). Nevertheless, OCS cannot view the deep space for the shelter of its solar sail, and the onboard calibration of TIR is performed periodically by heating the blackbody from normal temperature at about 293 ± 5 K to high temperature near 328 ± 5 K and imaging the blackbody at these two temperatures [6]. However, the normal temperature of blackbody cannot be controlled and measured exactly which leads to onboard calibration error of 0.90 K at least [7]. So it is necessary to substitute ground-based measurement result for the normal temperature point to reduce the calibration error.

$$L = \frac{DN - b}{g} \quad (1)$$

where DN is digital number, L is calibrated radiance, b and g are calibration coefficients of offset and gain, respectively. Onboard calibration coefficients b and g are obtained by two-point regression.

3. Field and campaigns

3.1. Lake Qinghai

Water body is used as an ideal calibration target for its uniformity in composition, high emissivity and low surface temperature variation (≤1 °C) over large area [8,9]. Lake Qinghai located at position (36.3°–37.0° N, 99.5°–100.7° E) in the Qinghai basin, west of China, is 150 km away from capital Xining of Qinghai province. This lake, which is the largest inland saltwater lake in China, is 105 km from east to west, and 63 km from north to south. Its average elevation is 3.196 km with a maximum water depth of about 38 m. It is in the typically dry and clean climate with aerosol optical depth and column water vapor lower than 0.1 and 2.0 cm almost throughout the year respectively [10]. Lake Qinghai is the primary thermal infrared calibration field in China for its surface condition, atmospheric qualification and accessibility that satisfy certain conditions of thermal site [11]. National Satellite Meteorological Center of China (NSMCC) has deployed three moored buoys at the site to measure and log the water bulk temperature with a thermistor at about 2–4 cm beneath the water surface all the year round except in winter. Fig. 1 shows the map of Lake Qinghai.

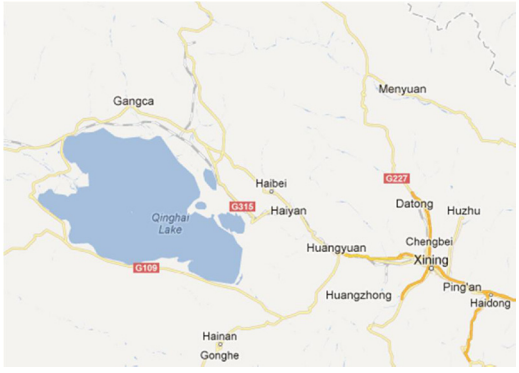

Fig. 1. Map of vicarious calibration site Lake Qinghai.

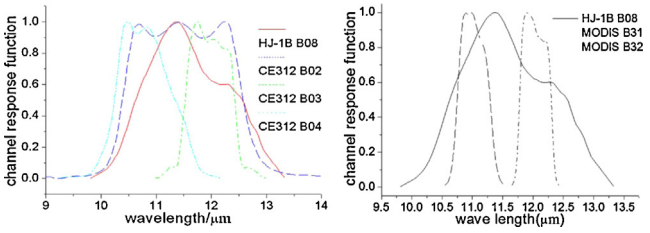

Fig. 2. Comparisons of CRFs in IRS B08, CE312 (left) and MODIS (right).

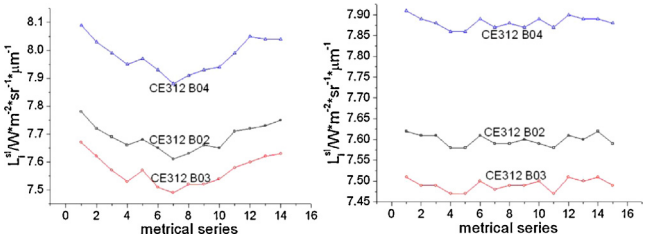

Fig. 3. CE312 surface-leaving radiance on 16 (left) and 19 (right) August.

3.2. Field campaigns

VC experiments for the TIR subsystem were regularly conducted by NSMCC, China Center for Resources Satellite Data and Application (CCRSDA), and Institute of Remote Sensing Applications of Chinese Academy of Sciences on 12–24 August, 2009. Water surface-leaving radiance was measured with a CIMEL CE312 radiometer that was accurately calibrated by a highly accurate field portable blackbody (Mikron M340) before and after the satellite overpass, and water bulk temperature was measured 2–3 cm beneath the surface simultaneously by thermometer. Fig. 2 gives the relative channel response function (CRF) of CIMEL CE312 B02, B03 and B04 compared to IRS B08. In addition to the *in situ* water measurements, multiple atmospheric sounding balloons were launched at the shore to provide air temperature and relative humidity profiles at the satellite overpass. Figs. 3 and 4 give the leaving water radiance and atmospheric profiles on 16 and 19 August, 2009, respectively.

4. Bands match and sensitivity analysis

4.1. Radiance-based method

The effective top of atmosphere (TOA) radiance observed by band i from satellite includes two parts, that is atmospheric

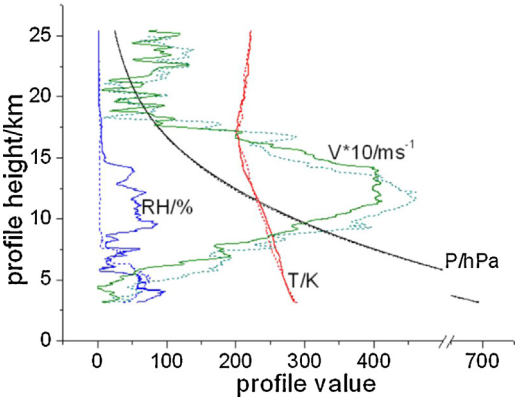

Fig. 4. Radiosonder profiles on 16 (dotted line) and 19 (straight line) August.

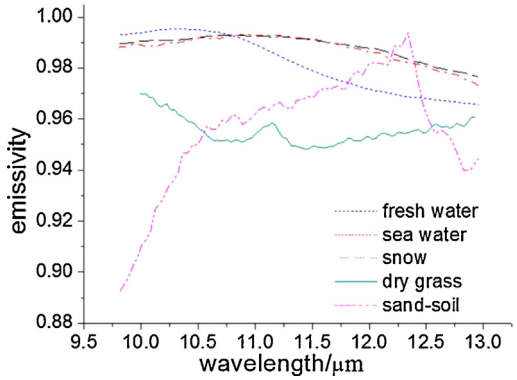

Fig. 5. Five emissivities selected from MODIS UCSB library.

upwelling emissive radiance and surface-leaving radiance attenuated by atmosphere as:

$$L_i^{\mathrm{TOA}} = \tau_i L_i^{\mathrm{sl}} + L_i^{\mathrm{up}} \tag{2}$$

where L_i^{sl} is the surface-leaving or at-surface radiance defined by

$$L_i^{\mathrm{sl}} = \frac{\int \left[\varepsilon(\lambda)B(\lambda,T) + (1-\varepsilon(\lambda))L^{\mathrm{down}}(\lambda)\right] f_i(\lambda)\,d\lambda}{\int f_i(\lambda)\,d\lambda} \tag{3}$$

and τ_i is atmospheric transmittance, L_i^{up} is atmospheric up-welling thermal radiance, $\varepsilon(\lambda)$ is site surface spectral emissivity, $B(\lambda, T)$ is Planck function, $L^{\mathrm{down}}(\lambda)$ is atmospheric spectral down-welling radiance, T is surface kinetic temperature, $f_i(\lambda)$ is relative channel response function.

In the temperature-based method, L_i^{TOA} is calculated by formulae (2) and (3) with measured field surface temperature and emissivity, whereas in the radiance-based method, L_i^{TOA} is calculated from formula (2) directly with deduced at-surface radiance that matched from at-surface radiance of reference band as

$$L_i^{\mathrm{sl}} = k_{\mathrm{ref}} L_{\mathrm{ref}}^{\mathrm{sl}} \tag{4}$$

where k_{ref} is band match factor, and $L_{\mathrm{ref}}^{\mathrm{sl}}$ is at-surface radiance of reference band measured in field with instrument such as CE312.

The atmospheric parameters (τ_i, L_i^{up} and $L^{\mathrm{down}}(\lambda)$) are calculated from atmospheric profiles by using a radiation transfer code such as MODTRAN [12,13].

4.2. Band match and sensitivity analysis

Band match factor k_{ref} is defined as below according to formulae (3) and (4):

$$k_{\mathrm{ref}} = \frac{L_i^{\mathrm{sl}}}{L_{\mathrm{ref}}^{\mathrm{sl}}} = \frac{\int \left[\varepsilon(\lambda)B(\lambda,T) + (1-\varepsilon(\lambda))L^{\mathrm{down}}(\lambda)\right] f_i(\lambda)\,d\lambda}{\int \left[\varepsilon(\lambda)B(\lambda,T) + (1-\varepsilon(\lambda))L^{\mathrm{down}}(\lambda)\right] f_{\mathrm{ref}}(\lambda)\,d\lambda} \frac{\int f_{\mathrm{ref}}(\lambda)\,d\lambda}{\int f_i(\lambda)\,d\lambda} \tag{5}$$

Estimated temperature T and emissivity ε were substituted for the real field measurements to figure out k_{ref}. Emissivities of five land surface types (shown as Fig. 5), in addition to blackbody ($\varepsilon = 1$), were chosen from the MODIS UCSB library to analysis their impacts on k_{ref} under different reference bands as CE312 B02, B03, and B04. Moreover, surface temperature was set up from 283 K to 305 K with sufficient interval to cover its actual value of field campaign. As a result, Figs. 6 and 7 give the results that convolved with atmospheric parameters on 16 and 19 August respectively.

The statistics of band match factor differences due to temperature and emissivity are shown as Table 2 according to Fig. 7. The

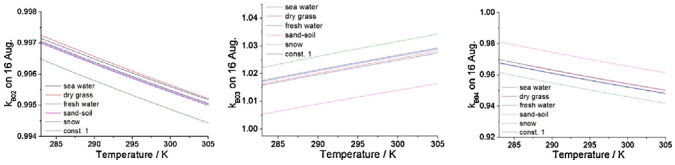

Fig. 6. Band match factors on 16 August CE312 B02, B03 and B04 as reference bands.

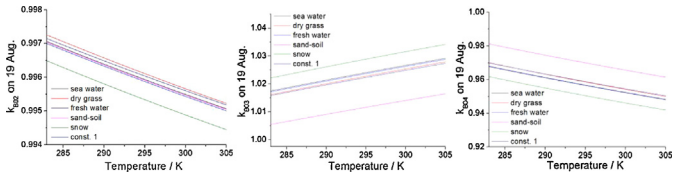

Fig. 7. Band match factors on 19 August CE312 B02, B03 and B04 as reference bands.

Table 2
Band match factor differences due to emissivity and temperature.

Differences (%)	k_{B02}		k_{B03}		k_{B04}	
	On 16	On 19	On 16	On 19	On 16	On 19
Due to ε	0.078	0.077	1.714	1.700	2.062	2.048
Due to T	0.201	0.202	1.142	1.143	2.078	2.080
Total	0.216	0.216	2.060	2.048	2.928	2.919

impacts due to emissivity and temperature on CE312 B02 can be ignored as they are less than 0.1 and 0.2 percent respectively, but their impacts on CE312 B03 and B04 exceed than 1.0 and 2.0 percent separately. Therefore, whether the impacts can be ignored depending not only on temperature and emissivity but also on CRFs themselves. For example, when the temperature estimated error is ±10 K, the impacts of estimation on CE312 B03 and B04 cannot be ignored for more than 1.1 and 2.0 percent even emissivity-specimens of fresh water, sea water and blackbody ($\varepsilon = 1$) were used as actual surface.

5. Data processing and error analysis

5.1. Surface-leaving radiance and temperature calculation

Surface-leaving radiance (SLR) of IRS B08 was calculated using formula (4) with field measurements and band match factors above as inputs. Then the radiance was converted to surface-leaving temperature (SLT) to facilitate comparison and analysis intuitively as shown in Fig. 8 plotted band by band, and the cross-band comparisons of each type emissivity are drawn in Fig. 9.

The impacts of both emissivity and temperature estimations on IRS B08 SLT are greatly different within three bands. B04 has the largest difference more than 1.8 K, B03 corresponding to 1.3 K, and B02 has the negligible difference of 0.14 K. Nevertheless, the SLT difference that using the average combination of band match factors of B03 and B04 is much smaller than that of B03 or B04 used alone, which is 0.3 K shown as the last column in Table 3.

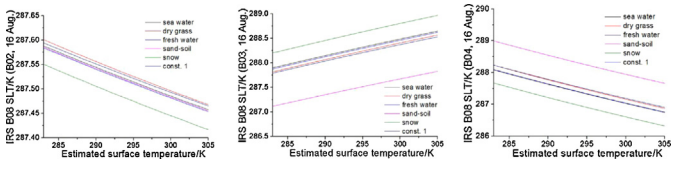

Fig. 8. Predicted surface-leaving temperature of IRS B08.

Table 3
Predicted SLTs differences due to emissivity and temperature.

Differences (K)	SLT(k_{B02})		SLT(k_{B03})		SLT(k_{B04})		SLT($k_{Avg.(B03,B04)}$)	
	On 16	On 19	On 16	On 19	On 16	On 19	On 16	On 19
Due to ε	0.05	0.05	1.11	1.10	1.33	1.32	0.11	0.11
Due to T	0.13	0.13	0.74	0.74	1.34	1.34	0.30	0.30
Total	0.14	0.14	1.34	1.33	1.89	1.88	0.31	0.32

Table 4
IRS B08 TOA radiances and differences due to emissivity and temperature.

Differences (%)	TOAR(k_{B02})		TOAR(k_{B03})		TOAR(k_{B04})		TOAR($k_{Avg.(B03,B04)}$)	
	On 16	On 19	On 16	On 19	On 16	On 19	On 16	On 19
	7.458	7.446	7.522	7.529	7.41	7.407	7.492	7.468
Due to ε	0.068	0.068	1.499	1.484	1.801	1.786	0.144	0.143
Due to T	0.176	0.176	0.999	0.998	1.815	1.813	0.397	0.396
Total	0.189	0.188	1.801	1.789	2.557	2.545	0.423	0.421

Note: TOAR unit: W m^{-2} μm^{-1} sr^{-1}, the same below.

Table 5
Comparison between MODIS B31, 32 and IRS B08 of TOAR.

Differences (%)	MODIS(B31)		MODIS(B32)		MODIS(Avg.(B31,B32))	
	On 16	On 19	On 16	On 19	On 16	On 19
	7.666	7.691	7.209	7.237	7.438	7.464
IRS B08(k_{B02})	2.79	3.29	3.45	2.89	0.27	0.24
IRS B08(k_{B03})	1.91	2.15	4.34	4.03	1.13	0.87
IRS B08(k_{B04})	3.45	3.83	2.79	2.35	0.38	0.77
IRS B08($k_{Avg.(B03,B04)}$)	2.32	2.98	3.93	3.19	0.73	0.05

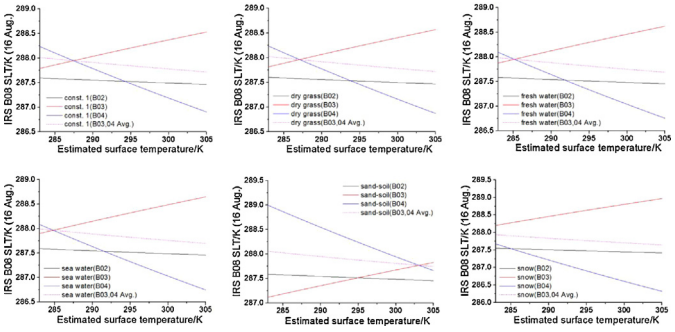

Fig. 9. Predicted SLT comparisons in tri-reference bands.

5.2. TOA radiance calculation and validation

The top of atmosphere radiance (TOAR) of IRS B08 was calculated by formula (2) with the SLR reckoned above, the atmospheric transmissivity and upwelling radiance of MODTRAN outputs. The differences due to emissivity and temperature are much smaller based on k_{B02} and $k_{Avg.(B03,B04)}$ than that of both k_{B03} and k_{B04} (Table 4).

The TOAR of IRS B08 was validated by comparing to those of TERRA/MODIS B31 and B32, and the comparison among their CRFs is shown in Fig. 2. The TOAR differences between IRS B08(k_{B02}) and MODIS(Avg.(B31,32)) are smaller than 0.3 percent on two days, corresponding to 0.25 K TOA temperature, while the differences between IRS B08($k_{Avg.(B03,B04)}$) and MODIS(Avg.(B31,32)) are 0.73 and 0.05 percent respectively on 16 and 19 shown as the last column in Table 5.

Table 6
Vicarious calibration coefficient update.

b (DN)	g (W^{-1} m^2 sr μm)
−13.19	58.79

6. Calibration coefficients update

The OCS carried out an on-board calibration on 14 August before the field campaign to provide the high temperature point data for this vicarious calibration. The calibration coefficients were updated by two point regression, the high temperature point of OCS on 14 August as the first one and the field campaign value that substituted for the normal temperature point of OCS as the other one. The vicarious calibration result in Table 6 could be used to calibrate the imagery from August 2009 to August 2010 after which a new vicarious calibration was implemented.

7. Discussion and conclusion

Radiance based method is simple in terms of field campaign and data processing compared to temperature based method, and do not need the synchronous measurement of field temperature and emissivity. The key factor of radiance based method that affected the precision is the difference of channel response functions between target and reference sensors. Therefore, it is necessary to perform band match in the calibration process and estimated its impacts on precision. Band match factor is obviously influenced by channel center wavelengths of target and reference bands for the variation of surface temperature and emissivity, and the closer distance the better accuracy. CE312 B02 is closer to IRS B08 than B03 and B04, and the differences of k_{03} and k_{04} due to estimations of temperature and emissivity are nearly 10 times of k_{02}, whose variation could be ignored as less than 0.22 percent. However, sometimes the center wavelength of target band is not close enough to that of reference bands to achieve the assigned calibration precision, thus the linear combination of two surrounding bands could be used to reduce the uncertainty that generated

evidently by either channel used alone. The average combination of CE312 B03 and B04 reduced the uncertainty of SLT from 1.34 K and 1.89 K to 0.32 K, respectively. The vicarious calibration accuracy based on CE312 B02 is 0.25 K and the vicarious calibration coefficients could be used from August 2009 to August 2010 after which a new field campaign was performed.

Acknowledgements

Project 41301388 supported by NSFC; Ph.D. Tianhai Chen for technological supports.

References

[1] M. Lefevre, O. Bauer, A. Iehle, et al., An automatic method for the calibration of time-series of Meteosat images, Int. J. Remote Sens. 21 (5) (2000) 1025–1045.
[2] P. Slater, S.F. Biggar, K. Thome, Vicarious radiometric calibrations of EOS sensors, J. Atmos. Ocean. Technol. 13 (1996) 349–359.
[3] K. Thome, K. Arai, H. Simon, et al., ASTER preflight and inflight calibration and the validation of level 2 products, IEEE Trans. Geosci. Remote Sens. 36 (4) (1998) 1161–1171.
[4] T. Hideyuki, D.P. Frank, J.H. Simon, et al., Vicarious calibration of ASTER thermal infrared bands, IEEE Trans. Geosci. Remote Sens. 43 (December (12)) (2005) 2733–2746.
[5] J.G. Li, X.F. Gu, T. Yu, et al., A twin-channel difference model for cross-calibration of thermal infrared band, Sci. China Technol. Sci. 55 (2012) 2048–2056.
[6] Q.J. Han, Q.Y. Fu, Z.Q. Pan, et al., Integrated radiometric calibration for the infrared multispectral camera of HJ-1B, Sci. China Technol. Sci. 41 (2011) 66–75.
[7] J.G. Li, X.F. Gu, T. Yu, Q.J. Han, et al., Lookup table method of effective bandwidth for HJ-1B B08 on-board radiometric calibration, J. Remote Sens. 15 (1) (2011) 60–72.
[8] R.S. John, J.A. Barsi, B.L. Nordgren, et al., Calibration of Landsat thermal data and application to water resource studies, Remote Sens. Environ. 78 (2001) 108–117.
[9] J.A. Barsi, J.R. Schott, F.D. Palluconi, et al., Landsat TM and ETM+ thermal band calibration, Remote Sens. 29 (2) (2003) 141–153.
[10] Y. Zhang, X.F. Gu, T. Yu, et al., Integrated radiometric calibration for IRMSS of CBERS-02, Sci. China Technol. Sci. 35 (2005) 70–88 (in Chinese).
[11] Z. Wan, Y. Zhang, X. Ma, et al., Vicarious calibration of the moderate resolution imaging spectroradiometer airborne simulator thermal-infrared channels, Appl. Opt. 38 (1999) 6294–6306.
[12] A. Berk, L.S. Bernstein, D.C. Robertson, MODTRAN: A Moderate Resolution Model for LOWTRAN-7. GL-TR-89-0122, Air Force Geophysics Laboratories, Hanscom Air Force Base, MA, 1989, pp. 28.
[13] J.M. Christopher, J.S. James, R.H. Andrew, A cross-calibration of GMS-5 thermal channels against ATSR-2, Remote Sens. Environ. 84 (2003) 268–282.